

Quantum properties of counter-propagating two-photon states generated in a planar waveguide.

Jan Peřina Jr.

Joint Laboratory of Optics of Palacký University and
Institute of Physics of Academy of Sciences of the Czech Republic,
17. listopadu 50A, 772 00 Olomouc, Czech Republic.

A nonlinear planar waveguide pumped by a beam orthogonal to its surface may serve as a versatile source of photon pairs. Changing pump-pulse duration, pump-beam transverse width, and angular decomposition of pump-beam frequencies characteristics of a photon pair including spectral widths of signal and idler fields, their time durations as well as degree of entanglement of two fields can be changed significantly. Using the measured spectral widths of the down-converted fields and width of a coincidence-count dip in a Hong-Ou-Mandel interferometer entropy of entanglement can be determined.

PACS numbers: 42.50.Dv Quantum optics, 42.65.Wi Nonlinear waveguides, 42.65.Lm Parametric down-conversion and production of entangled photons

I. INTRODUCTION

The process of spontaneous parametric down-conversion as a source of entangled photon pairs has been used in numerous experiments during the last twenty years. The physicists went through a long way from the first pioneering experiments showing basic properties of entangled photon pairs [spectral (temporal) and polarization correlations of photons comprising a pair, see, e.g. [1, 2]] to the recent sophisticated experimental setups that demonstrate quantum teleportation [3], quantum cloning [4], test Bell and other nonclassical inequalities [5, 6], or generate Greenberger-Horne-Zeilinger states [7]. Usefulness of the fragile entangled photon pairs has also been verified in applications like quantum cryptography [8] and absolute metrology [9] to name a few.

Also sources of photon pairs have been improved significantly. Various geometric configurations of usual nonlinear crystals (see, e.g., in [10, 11]) are gradually being replaced by new more efficient sources based on quasi-phase-matching [12, 13, 14, 15]. Nonlinear photonic-band-gap fibers seem to be extraordinarily interesting as sources of photon pairs (emerging in the process of four-wave mixing) due to a high effective nonlinearity [16, 17]. Nonlinear layered structures as sources of photon pairs are under investigation at present [18, 19].

A great deal of attention has been devoted to the generation of two-photon states with specific spectral properties in bulk materials. Entangled two-photon states with coincident frequencies have been obtained using extended phase-matching conditions, i.e. assuming group-velocity phase matching on the top of the usual phase matching [20, 21, 22]. Such states have perfect visibility in the usual interferometric setups and moreover allow a very precise clock synchronization [23]. Spectrally uncorrelated two-photon states have also been studied extensively because they seem to be extraordinarily useful for linear quantum computation that needs indistinguishable photons with a perfect time synchronization

[24, 25]. Although such states can be generated from usual bulk crystals for suitable crystal length and pump-beam waist in non-collinear configurations [26, 27], more flexible approaches have been suggested in [24] exploiting phase-matching in the transverse plane. Both coincident-frequency entangled and unentangled two-photon states can be obtained in a nonlinear crystal with achromatic phase matching, i.e. when pump-beam frequencies are decomposed such that every frequency propagates along a slightly different angle [28, 29]. Also the so-called nonlinear crystal superlattices, i.e. structures composed of several identical pieces of nonlinear material and spacers, have provided additional degrees of freedom for tailoring properties of the generated two-photon states [30, 31]. Results appropriate for photonic-band gap structures [32] are reached for a higher number of nonlinear pieces.

Also planar nonlinear structures are promising as sources of entangled photon pairs because, using specific geometric configurations, they provide large possibilities for tailoring properties of the generated photon pairs. One of the most perspective configurations (suggested and elaborated in [33, 34, 35, 36]) is based upon pumping a planar waveguide by a beam perpendicular to its surface. Signal and idler photons then emerge as counter-propagating guided waves. Disadvantage of this configuration is that the pump beam propagates through a very thin nonlinear medium which thickness is given by the depth of the waveguide. In order to suppress destructive interference in the three-wave nonlinear process this thickness has to be of the order of pump-field wavelength. Thus, very low generation rates have to be expected. To cope with a low efficiency of the nonlinear process more sophisticated structures have been suggested [37, 38]. They use Bragg mirrors both above and below the waveguide. Their properties are chosen such that the pump-beam electric-field amplitude is maximally enhanced inside the nonlinear waveguide. This may result in enhancement of the efficiency by several orders of magnitude. The first experimental demonstration of

this source has been already reported in [39]. The use of pump pulses with frequencies propagating along different angles brings even more flexibility and so photon pairs with an arbitrary shape of a two-photon spectral amplitude can be generated [40].

As shown in this paper using a simple model of planar waveguide with parabolic index of refraction [35, 41], properties of photon pairs (spectral and temporal widths of the down-converted fields and entanglement) generated from this type of geometry can be modified in broad ranges simply by changing parameters of the pump beam (pump-pulse duration, pump-beam transverse width, angular decomposition of pump-beam frequencies). Spectral widths of the down-converted fields can spread from circa 1 nm up to several tens of nm. Spectrally uncorrelated (separable) states as well as strongly entangled states can be observed. A method for the determination of entropy of entanglement from the measured signal- and idler-field intensity spectra and width of the coincidence-count pattern in a Hong-Ou-Mandel interferometer is also suggested.

The paper is organized as follows. Sec. II is devoted to the determination of a two-photon spectral amplitude of the generated photon pair. This amplitude is later used to derive spectral (Sec. III) and temporal (Sec. IV) properties of the down-converted fields, and characterize entanglement of the signal and idler fields (Sec. V). Experimental determination of entropy of entanglement is discussed in Sec. VI. Conclusions are drawn in Sec. VII. Appendix A contains general formulas describing properties of photon pairs. Appendix B is devoted to Schmidt decomposition of a two-photon spectral amplitude.

II. TWO-PHOTON SPECTRAL AMPLITUDE OF A PHOTON PAIR GENERATED FROM A WAVEGUIDE

We consider the generation of a photon-pair into guided modes of a planar waveguide made of LiNbO₃ that is pumped by a travelling-wave pump beam at the wavelength $\lambda_p = 1.064 \times 10^{-6}$ m that propagates under the central angle θ_p^0 with respect to the x axis orthogonal to the surface (see Fig. 1). The pump beam is assumed not to be cross spectrally pure in general, i.e. different pump-beam frequencies can propagate under different propagation angles. The guided signal and idler fields then form counter-propagating beams. For simplicity, we pay attention to the waveguide with a parabolic profile of index of refraction $n(x)$, $n(x)^2 = n_0^2(1 - \alpha^2 x^2)$ (α is parameter of the waveguide) that supports only TE-guided modes with a gaussian profile.

Energy of the nonlinear interaction that produces photon pairs is described by Hamiltonian \hat{H} :

$$\hat{H}(t) = \epsilon_0 d \int dV \left[E_p^{(+)}(\mathbf{r}, t) \hat{E}_s^{(-)}(\mathbf{r}, t) \hat{E}_i^{(-)}(\mathbf{r}, t) + \text{h.c.} \right], \quad (1)$$

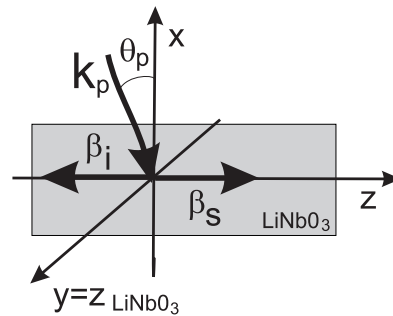


FIG. 1: Sketch of a nonlinear planar waveguide made of LiNbO₃ with parabolic profile of index of refraction along the x axis. The optical axis of LiNbO₃ as well as polarization directions of signal, idler, and pump fields are parallel to the y axis. The signal (idler) field propagates along the $+z$ ($-z$) axis with propagation constant β_s (β_i); the pump field with central wave-vector k_p^0 propagates under central angle θ_p^0 with respect to the x axis. The waveguide is confined into the region $(-L_y/2, L_y/2)$ in y direction.

where $E_p^{(+)}$ is positive-frequency part of the pump-beam electric-field amplitude and $\hat{E}_s^{(-)}$ ($\hat{E}_i^{(-)}$) stands for negative-frequency part of the signal- (idler-) beam electric-field amplitude operator. Symbol ϵ_0 denotes permittivity of vacuum, d is effective second-order nonlinear coefficient, and h.c. means a hermitian conjugated term. Integration in Eq. (1) is over interaction volume V .

In the considered waveguide, positive-frequency parts of the signal- and idler-beam electric-field amplitude operators $\hat{E}_s^{(+)}$ and $\hat{E}_i^{(+)}$ can be decomposed as $[E_p^{(+)} = (E_p^{(+)})^\dagger]$:

$$\begin{aligned} \hat{E}_a^{(+)}(\mathbf{r}, t) &= \int d\omega_a e_a(\mathbf{r}, \omega_a) \hat{a}_a(\omega_a), \\ e_a(\mathbf{r}, \omega_a) &= C_a(\omega_a) \text{rect}_{(-L_y/2, L_y/2)}(y) \\ &\quad \times \exp\left(-\frac{\gamma_a^2 x^2}{2}\right) \exp(\pm i\beta_a z) \exp(-i\omega_a t), \\ |C_a(\omega_a)|^2 &= \frac{\hbar\omega_a\gamma_a}{2\sqrt{\pi}\epsilon_0 n_0^3(\omega_a) c L_y}, \quad a = s, i; \end{aligned} \quad (2)$$

symbol $\hat{a}_a(\omega_a)$ denotes annihilation operator of a mode with frequency ω_a in field a . The sign $+$ ($-$) in the second relation in Eq. (2) is for the signal (idler) field that propagates along the $+z$ ($-z$) axis. In Eq. (2), $n_0(\omega_a)$ is index of refraction of field a with frequency ω_a , c means speed of light in vacuum, \hbar reduced Planck constant, L_y width of the waveguide along the y axis where a rectangular profile is assumed, and $\gamma_a(\omega_a) = \sqrt{n_0(\omega_a)\omega_a\alpha/c}$. Function $\text{rect}_{(a,b)}(x)$ equals 1 for $a < x < b$ and is zero otherwise. Normalization constant C_a in Eq. (2) has been determined from the condition that a photon emitted into a guided mode has energy $\hbar\omega_a$:

$$2\epsilon_0 n_0^2(\omega_a) \int dV |e_a(\mathbf{r}, \omega_a)|^2 = \hbar\omega_a, \quad a = s, i. \quad (3)$$

We assume that the interaction volume V has ‘length’

$c/n_0(\omega_a^0)$ along the z axis when determining constant C_a in Eq. (2).

Propagation constant β_a of field a along the z axis is given as follows (for details, see [41]):

$$\beta_a(\omega_a) = \frac{n_0(\omega_a)\omega_a}{c} \sqrt{1 - \frac{\alpha c}{n_0(\omega_a)\omega_a}}. \quad (4)$$

It can be approximately expressed as:

$$\begin{aligned} \beta_a(\omega_a) &= \beta_a^0 + \frac{\omega_a - \omega_a^0}{v_a}, \\ \beta_a^0 &= \beta_a(\omega_a^0), \\ \frac{1}{v_a} &= \left. \frac{d\beta_a}{d\omega_a} \right|_{\omega_a=\omega_a^0}, \end{aligned} \quad (5)$$

where v_a denotes group velocity of field a .

The travelling-wave pump beam with central frequency ω_p^0 and propagating along central angle θ_p^0 is assumed to have a gaussian profile along the y and z axes characterized by widths Y_p and Z_p , respectively, and is also gaussian in the time domain with pump-pulse duration τ_p and chirp parameter a_p . Different monochromatic components of the pump beam can propagate along different angles $\theta_p(\omega_p)$, e.g. as a consequence of pump-beam reflection on an optical grating or after propagation through a prism. The pump-beam positive-frequency electric-field amplitude $E_p^{(+)}$ can be written in the form:

$$\begin{aligned} E_p^{(+)}(\mathbf{r}, t) &= \frac{1}{\sqrt{2\pi}} \int d\omega_p E_p^{(+)}(\mathbf{r}, \omega_p) \exp(-i\omega_p t), \\ E_p^{(+)}(\mathbf{r}, \omega_p) &= C_p(\omega_p) \exp\left(-\frac{z^2}{Z_p^2}\right) \exp\left(-\frac{y^2}{Y_p^2}\right) \\ &\quad \times \exp[ik_p \sin(\theta_p(\omega_p))z] \exp[-ik_p \cos(\theta_p(\omega_p))x] \\ &\quad \times \exp\left[-\frac{\tau_p^2(\omega_p - \omega_p^0)^2}{4(1 + ia_p)}\right], \\ |C_p(\omega_p)|^2 &= \frac{\tau_p}{\sqrt{2\pi}\pi\epsilon_0 n_0^2(\omega_p) Y_p Z_p (1 + a_p^2)} \frac{P_p}{v_p \cos(\theta_p(\omega_p)) f}, \end{aligned} \quad (6)$$

v_p is pump-field group velocity [$k_p(\omega_p) = k_p^0 + (\omega_p - \omega_p^0)/v_p$, $k_p^0 = k_p(\omega_p^0)$, $1/v_p = dk_p/d\omega_p|_{\omega_p=\omega_p^0}$], P_p pump-field power, and f denotes repetition rate of the pulsed pump field.

First-order perturbation solution of the Schrödinger equation using Hamiltonian $H(t)$ given in Eq. (1) and assuming the incident signal and idler fields in vacuum states provides the following expression for an outgoing two-photon state $|\psi^{(2)}\rangle$:

$$|\psi^{(2)}\rangle = \int d\omega_s \int d\omega_i \Phi^{1p}(\omega_s, \omega_i) \hat{a}_s^\dagger(\omega_s) \hat{a}_i^\dagger(\omega_i) |\text{vac}\rangle. \quad (7)$$

Two-photon spectral amplitude $\Phi^{1p}(\omega_s, \omega_i)$ giving the probability amplitude of having a signal photon at frequency ω_s and an idler photon at frequency ω_i generated

from one pump pulse is derived in the form:

$$\begin{aligned} \Phi^{1p}(\omega_s, \omega_i) &= -i \frac{\sqrt{2\pi} 2\pi^2 \epsilon_0 d}{\hbar} C_p(\omega_s + \omega_i) C_s^*(\omega_s) C_i^*(\omega_i) \\ &\quad \times \frac{Y_p Z_p}{\sqrt{\gamma_s^2 + \gamma_i^2}} \text{erf}\left(\frac{L_y}{2Y_p}\right) \exp\left[-\frac{\tau_p^2(\omega_s + \omega_i - \omega_p^0)^2}{4(1 + ia_p)}\right] \\ &\quad \times \exp\left[-\frac{Z_p^2[k_p \sin(\theta_p(\omega_s + \omega_i)) - \beta_s + \beta_i]^2}{4}\right] \\ &\quad \times \exp\left[-\frac{k_p^2 \cos^2(\theta_p(\omega_s + \omega_i))}{2(\gamma_s^2 + \gamma_i^2)}\right]; \end{aligned} \quad (8)$$

symbol erf stands for error function [$\text{erf}(x) = 2/\sqrt{\pi} \int_0^x \exp(-y^2) dy$].

Using first-order Taylor expansions for propagation constants k_p , β_s , and β_i as well as for propagation angle θ_p together with second-order Taylor expansion for the expression $1/(\gamma_s^2 + \gamma_i^2)$ [$1/(\gamma_s^2 + \gamma_i^2) \approx g_0 + g_{1s}\Delta\omega_s + g_{1i}\Delta\omega_i + g_{2s}\Delta\omega_s^2 + g_{2i}\Delta\omega_i^2 + g_{2si}\Delta\omega_s\Delta\omega_i$, $\Delta\omega_a = \omega_a - \omega_a^0$, $a = s, i$] we arrive at a two-photon spectral amplitude Φ giving contribution from f pump pulses and having the following gaussian form:

$$\begin{aligned} \Phi(\omega_s, \omega_i) &= C_\Phi \sqrt{\frac{Z_p \tau_p}{1 + a_p^2}} \exp[-\phi(\omega_s, \omega_i)], \\ \phi(\omega_s, \omega_i) &= f_{2s}\Delta\omega_s^2 + f_{2i}\Delta\omega_i^2 + f_{2si}\Delta\omega_s\Delta\omega_i \\ &\quad + f_{1s}\Delta\omega_s + f_{1i}\Delta\omega_i + f_0. \end{aligned} \quad (9)$$

Coefficients f occurring in Eq. (9) are expressed as follows:

$$\begin{aligned} f_{2a} &= \frac{\tau_p^2}{4(1 + ia_p)} + \frac{V_{pa}^2 Z_p^2}{4} + \frac{1}{\sigma_a^2} + \mathcal{G}_a, \\ \mathcal{G}_a &= \frac{k_p^0 \cos(\theta_p^0)}{2} \left(k_p^0 \cos(\theta_p^0) g_{2a} \right. \\ &\quad + 2 \left[\frac{\cos(\theta_p^0)}{v_p} - k_p^0 \sin(\theta_p^0) \tilde{D}_{\theta_p} \right] g_{1a} \\ &\quad + \left[\frac{\cos(\theta_p^0)}{k_p^0 v_p^2} - \frac{4 \sin(\theta_p^0)}{v_p} \tilde{D}_{\theta_p} \right. \\ &\quad \left. \left. - \frac{k_p^0 \cos(2\theta_p^0)}{\cos(\theta_p^0)} \tilde{D}_{\theta_p}^2 \right] g_0 \right), \end{aligned}$$

$$a = s, i,$$

$$f_{2si} = \frac{\tau_p^2}{2(1 + ia_p)} + \frac{V_{ps} V_{pi} Z_p^2}{2} + \frac{1}{\sigma_a^2} + \mathcal{G}_{si},$$

$$\begin{aligned} \mathcal{G}_{si} &= \frac{k_p^0 \cos(\theta_p^0)}{2} \left(k_p^0 \cos(\theta_p^0) g_{2si} \right. \\ &\quad + 2 \left[\frac{\cos(\theta_p^0)}{v_p} - k_p^0 \sin(\theta_p^0) \tilde{D}_{\theta_p} \right] (g_{1s} + g_{1i}) \\ &\quad + 2 \left[\frac{\cos(\theta_p^0)}{k_p^0 v_p^2} - \frac{4 \sin(\theta_p^0)}{v_p} \tilde{D}_{\theta_p} \right. \end{aligned}$$

$$\begin{aligned}
& - \frac{k_p^0 \cos(2\theta_p^0)}{\cos(\theta_p^0)} \tilde{D}_{\theta_p}^2 \Big] g_0 \Big), \\
& \qquad \qquad \qquad a = s, i, \\
f_{1a} &= k_p^0 \cos(\theta_p^0) \left(\frac{k_p^0 \cos(\theta_p^0)}{2} g_{1a} \right. \\
& \quad \left. + \left[\frac{\cos(\theta_p^0)}{v_p} - k_p^0 \sin(\theta_p^0) \tilde{D}_{\theta_p} \right] g_0 \right), \quad a = s, i, \\
f_0 &= \frac{[k_p^0 \cos(\theta_p^0)]^2}{2} g_0, \tag{10}
\end{aligned}$$

and

$$\begin{aligned}
V_{ps} &= \frac{\sin(\theta_p^0)}{v_p} + k_p^0 \cos(\theta_p^0) \tilde{D}_{\theta_p} - \frac{1}{v_s}, \\
V_{pi} &= \frac{\sin(\theta_p^0)}{v_p} + k_p^0 \cos(\theta_p^0) \tilde{D}_{\theta_p} + \frac{1}{v_i}. \tag{11}
\end{aligned}$$

Coefficient \tilde{D}_{θ_p} describes angular decomposition of pump-beam frequencies; $\tilde{D}_{\theta_p} = d\theta_p(\omega_p)/d\omega_p|_{\omega_p=\omega_p^0}$; $D_{\theta_p} = \tilde{D}_{\theta_p}(\omega_p^0)^2/(2\pi c)$. Influence of frequency filters with a gaussian shape is described by their widths σ_s and σ_i (for the signal and idler fields, respectively) that occur in Eq. (10).

Normalization constant C_Φ introduced in Eq. (9) is determined along the expression:

$$\begin{aligned}
|C_\phi|^2 &= \frac{\sqrt{2\pi}\pi^2 d^2 \omega_s^0 \omega_i^0}{\epsilon_0 c^2 n_0^2(\omega_p^0) n_0^3(\omega_s^0) n_0^3(\omega_i^0)} \frac{\sqrt{n_0(\omega_s^0) n_0(\omega_i^0) \omega_s^0 \omega_i^0}}{n_0(\omega_s^0) \omega_s^0 + n_0(\omega_i^0) \omega_i^0} \\
&\quad \times \frac{Y_p}{L_y^2} \text{erf}^2 \left(\frac{L_y}{2Y_p} \right) \frac{P_p}{v_p \cos(\theta_p^0)}. \tag{12}
\end{aligned}$$

Phase matching for central frequencies has been assumed when deriving the expression for two-photon spectral amplitude Φ written in Eq. (9), i.e.

$$k_p^0 \sin(\theta_p^0) - \beta_s^0 + \beta_i^0 = 0. \tag{13}$$

Equation (13) represents condition for possible values of central frequencies ω_p^0 , ω_s^0 , ω_i^0 and central angle θ_p^0 of pump-beam propagation. This condition even with the inclusion of quasi-phase matching has been extensively studied in [35].

The role of pump-pulse duration τ_p and pump-beam transverse width Z_p on the shape of two-photon spectral amplitude Φ can be understood when we transform the amplitude Φ into new variables Ω and ω ; $\Omega = (\omega_s + \omega_i)/2$, $\omega = (\omega_s - \omega_i)/2$:

$$\begin{aligned}
\Phi(\Omega, \omega) &= 2C_\phi \sqrt{\frac{Z_p \tau_p}{1 + a_p^2}} \\
&\quad \times \exp \left\{ - \left[\frac{\tau_p^2}{1 + ia_p} + \frac{Z_p^2 (V_{ps} + V_{pi})^2}{4} + \frac{1}{\sigma_+^2} \right] \Delta\Omega^2 \right. \\
&\quad \left. + \left[\frac{Z_p^2 (V_{ps} + V_{pi}) V_{si}}{2} - \frac{2}{\sigma_-^2} \right] \Delta\Omega \Delta\omega \right\},
\end{aligned}$$

$$- \left[\frac{Z_p^2 V_{si}^2}{4} + \frac{1}{\sigma_+^2} \right] \Delta\omega^2 \Big\}, \tag{14}$$

where

$$V_{si} = \frac{1}{v_s} + \frac{1}{v_i}, \tag{15}$$

$$\begin{aligned}
\frac{1}{\sigma_+^2} &= \frac{1}{\sigma_s^2} + \frac{1}{\sigma_i^2}, \\
\frac{1}{\sigma_-^2} &= \frac{1}{\sigma_s^2} - \frac{1}{\sigma_i^2}. \tag{16}
\end{aligned}$$

Coefficients \mathcal{G}_s , \mathcal{G}_i , and \mathcal{G}_{si} occurring in Eq. (10) have been neglected when the expression in Eq. (14) has been derived because they are small in comparison with those written explicitly in Eq. (14) under the studied conditions. We can see from Eq. (14) that pump-pulse duration τ_p influences only the coefficient of quadratic form in sum frequency Ω , whereas pump-beam transverse width Z_p and widths of spectral filters σ_s and σ_i modify all of them. The shape of a two-photon amplitude Φ can also be controlled using parameter \tilde{D}_{θ_p} of angular decomposition of pump-beam frequencies that occurs in expressions for the coefficients multiplying $\Delta\Omega^2$ and $\Delta\Omega\Delta\omega$ in Eq. (14). Nonzero values of parameter \tilde{D}_{θ_p} lead to rotation of the shape of the two-photon amplitude Φ in the plane spanned by frequencies ω_s and ω_i [28, 29].

Considering frequency degenerate case ($\omega_s^0 = \omega_i^0$, i.e. $v_s = v_i$ and $\theta_p^0 = 0$), cross spectrally pure pump beam ($\tilde{D}_{\theta_p} = 0$), and omitting frequency filters ($\sigma_s, \sigma_i \rightarrow \infty$) we obtain the two-photon spectral amplitude Φ in a simple form:

$$\begin{aligned}
\Phi(\Omega, \omega) &= 2C_\phi \sqrt{\frac{Z_p \tau_p}{1 + a_p^2}} \\
&\quad \times \exp \left[- \frac{\tau_p^2}{1 + ia_p} \Delta\Omega^2 - \frac{Z_p^2 V_{si}^2}{4} \Delta\omega^2 \right]; \tag{17}
\end{aligned}$$

i.e. pump-pulse duration τ_p determines properties depending on sum frequency Ω whereas pump-beam transverse width Z_p is responsible for properties related to difference frequency ω . This behavior is similar to that occurring in coincident-frequency entangled two-photon states generated from bulk materials and described, e.g., in [20] (length L of a crystal plays the role of Z_p).

III. SPECTRAL PROPERTIES OF PHOTON PAIRS, PHOTON-PAIR GENERATION RATE

Number N of photon pairs generated in 1 s is determined along the formula:

$$N = \int_{-\infty}^{\infty} d\omega_s \int_{-\infty}^{\infty} d\omega_i |\Phi(\omega_s, \omega_i)|^2. \tag{18}$$

The general expression for the number N of photon pairs assuming the spectral two-photon amplitude Φ in the

form written in Eq. (9) can be found in Appendix A [Eq. (A1)]. Neglecting coefficients \mathcal{G}_s , \mathcal{G}_i , and \mathcal{G}_{si} in Eq. (10), a simplified expression can be derived:

$$N = |C_\Phi|^2 \frac{\pi Z_p \tau_p}{(1 + a_p^2) \sqrt{D_{fr}}}, \quad (19)$$

where

$$D_{fr} = \frac{4}{\sigma_s^2 \sigma_i^2} + \frac{\tau_p^2}{(1 + a_p^2)} \left(\frac{1}{\sigma_s^2} + \frac{1}{\sigma_i^2} \right) + \frac{\tau_p Z_p^2 V_{si}^2}{4(1 + a_p^2)} + \frac{Z_p^2 V_{pi}^2}{\sigma_s^2} + \frac{Z_p^2 V_{ps}^2}{\sigma_i^2}. \quad (20)$$

If frequency filters are omitted, the expression in Eq. (19) for photon-pair generation rate N gets a simple form:

$$N = |C_\Phi|^2 \frac{2\pi^2}{\sqrt{1 + a_p^2 V_{si}}}, \quad (21)$$

i.e. the generation rate N does not depend both on pump-pulse duration τ_p and pump-beam transverse width Z_p . This is a consequence of geometry of the considered three-mode interaction. Assuming values of the waveguide parameters as written in Fig. 2 and incident pump-field power $P_p = 1$ W, the generation rate N equals 3×10^4 s⁻¹, i.e. if the pulsed pumping has repetition rate $f = 8 \times 10^7$ s⁻¹, a photon pair is generated from one pump pulse with probability 3.8×10^{-4} . Taking into account the depth of the waveguide of the order of pump-field wavelength, this probability is high. There are two reasons. The nonlinear process exploits the largest element of the nonlinear tensor d of LiNbO₃ (this gives 2 orders of magnitude in comparison with commonly used orientations). Also the down-converted fields are confined in their transverse profiles into very narrow regions, so the electric-field amplitude per one photon is high which improves efficiency of the nonlinear process.

Signal-field intensity spectrum S_s determined according to the formula

$$S_s(\omega_s) = \hbar \omega_s \int_{-\infty}^{\infty} d\omega_i |\Phi(\omega_s, \omega_i)|^2 \quad (22)$$

takes a gaussian form:

$$S_s(\omega_s) = s_s \exp \left[-\frac{(\omega_s - \omega_s^0 - \delta\omega_s^0)^2}{\sigma_{\omega_s}^2} \right]. \quad (23)$$

Amplitude s_s , width σ_{ω_s} , and shift $\delta\omega_s^0$ of the center for the signal-field intensity spectrum assuming negligible coefficients \mathcal{G}_s , \mathcal{G}_i , and \mathcal{G}_{si} are given as:

$$s_s = |C_\Phi|^2 \exp(-2f_0) \frac{\sqrt{\pi} \hbar \omega_s^0 \tau_p Z_p}{1 + a_p^2} \times \left[\frac{\tau_p^2}{2(1 + a_p^2)} + \frac{2}{\sigma_i^2} + \frac{Z_p^2 V_{pi}^2}{2} \right]^{-1/2}, \quad (24)$$

$$\sigma_{\omega_s} = \sqrt{\frac{\tau_p^2}{2(1 + a_p^2)} + \frac{2}{\sigma_i^2} + \frac{Z_p^2 V_{pi}^2}{2}} D_{fr}^{-1/2}, \quad (25)$$

$$\delta\omega_s^0 = 0; \quad (26)$$

D_{fr} is given in Eq. (20). The general expressions for parameters s_s , σ_{ω_s} , and $\delta\omega_s^0$ can be found in Appendix A [Eqs. (A4–A6)]. Characteristics of a gaussian idler-field intensity spectrum $S_i(\omega_i)$ can be derived from symmetry. When frequency filters are not included, the expression in Eq. (25) for width σ_{ω_s} can be further simplified:

$$\sigma_{\omega_s} = \frac{\sqrt{2}}{V_{si}} \sqrt{\frac{1}{Z_p^2} + \frac{(1 + a_p^2) V_{pi}^2}{\tau_p^2}}. \quad (27)$$

This means that the signal-field spectral width σ_{ω_s} (and similarly the idler-field spectral width σ_{ω_i}) decreases with increasing pump-pulse duration τ_p and pump-beam transverse width Z_p . Assuming cw pumping, spectral widths $\sigma_{\omega_s}^{\text{cw}}$ and $\sigma_{\omega_i}^{\text{cw}}$ are inversely proportional to pump-beam transverse width Z_p ;

$$\sigma_{\omega_s}^{\text{cw}} = \sigma_{\omega_i}^{\text{cw}} = \frac{\sqrt{2}}{V_{si} Z_p}. \quad (28)$$

On the other hand the following expressions hold for the pump-beam transverse width Z_p sufficiently large,

$$\begin{aligned} \sigma_{\omega_s} |_{Z_p \rightarrow \infty} &= \frac{\sqrt{2} |V_{pi}|}{V_{si}} \frac{\sqrt{1 + a_p^2}}{\tau_p}, \\ \sigma_{\omega_i} |_{Z_p \rightarrow \infty} &= \frac{\sqrt{2} |V_{ps}|}{V_{si}} \frac{\sqrt{1 + a_p^2}}{\tau_p}, \end{aligned} \quad (29)$$

i.e. widths σ_{ω_s} and σ_{ω_i} are inversely proportional to pump-pulse duration τ_p . Dependence of the width σ_{λ_s} of the signal-field intensity spectrum [$\sigma_{\lambda_s} = 2\pi c / (\omega_s^0)^2 \sigma_{\omega_s}$] on pump-pulse duration τ_p and pump-beam transverse width Z_p is shown in Fig. 2 for the considered waveguide. Narrow spectra broad circa 1 nm are generated if pump-pulse duration τ_p is sufficiently long and also pump-beam transverse width Z_p sufficiently wide. On the other hand, intensity spectra wide several tens of nm can be observed for ultrashort pump-pulses and strongly focused pump beams. The reason for this behavior is that shortening of a pump pulse and focusing of a pump beam lead to weakening of frequency and phase matching conditions.

Ratio $\sigma_{\omega_s} / \sigma_{\omega_i}$ of spectral widths of the signal- and idler-field intensities is important in some applications [24]. For example, photon pairs used in heralded single-photon sources should preferably be composed of one photon with a narrow spectrum (convenient in propagation through an optical fiber) and one photon with a wide spectrum (leading to high detection efficiencies when post-selecting). Provided that the pump beam is cross spectrally pure, the ratio $\sigma_{\omega_s} / \sigma_{\omega_i}$ is given by material constants (group velocities of three fields) for given values of pump-pulse duration τ_p and pump-beam transverse width Z_p . The ratio $\sigma_{\omega_s} / \sigma_{\omega_i}$ equals 1 if the signal

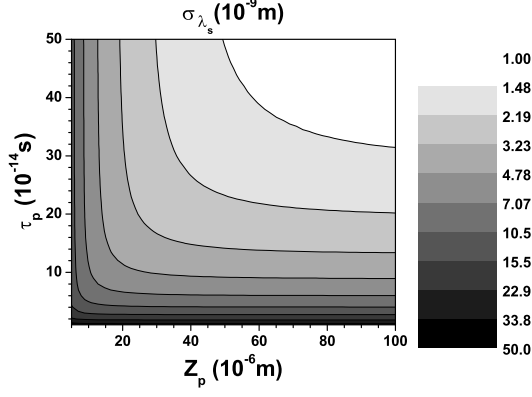


FIG. 2: Contour plot of width σ_{λ_s} of the signal-field intensity spectrum as a function of pump-pulse duration τ_p and pump-beam transverse width Z_p is shown; logarithmic scale is used on the z axis; $\lambda_p^0 = 1.064 \times 10^{-6}$ m, $\lambda_s^0 = \lambda_i^0 = 0.532 \times 10^{-6}$ m, $P_p = 1$ W, $a_p = 0$, $Y_p = 1 \times 10^{-5}$ m, $L_y = 1 \times 10^{-5}$ m, $D_{\theta_p} = 0$ deg m^{-1} , $\alpha = 4 \times 10^6$ m^{-1} , $\sigma_s = \sigma_i \rightarrow \infty$, $d = 41.05 \times 10^{-12}$ mV^{-1} .

and idler fields are symmetric ($\omega_s^0 = \omega_i^0$). On the other hand, parameter \tilde{D}_{θ_p} characterizing angular decomposition of pump-beam frequencies can substantially change this ratio. Either narrowing or broadening of an intensity spectrum of a down-converted field can be reached by the change of values of parameter \tilde{D}_{θ_p} , as formulas in Eqs. (27) and (11) indicate. Values around 10 for the ratio $\sigma_{\omega_s}/\sigma_{\omega_i}$ can be obtained for the waveguide with values of parameters defined in Fig. 2, as documented in Fig. 3. We note that high values of this ratio occur when the two-photon spectral amplitude Φ is nearly spectrally uncorrelated (compare Fig. 8 later).

IV. TEMPORAL PROPERTIES OF PHOTON PAIRS

Temporal properties of photon pairs can be conveniently described using two-photon amplitude Φ in the time domain that is given as a Fourier transform of that in the frequency domain:

$$\Phi(\tau_s, \tau_i) = \frac{1}{2\pi} \int_{-\infty}^{\infty} d\omega_s \int_{-\infty}^{\infty} d\omega_i \Phi(\omega_s, \omega_i) \times \exp(-i\omega_s \tau_s) \exp(-i\omega_i \tau_i). \quad (30)$$

Because the two-photon spectral amplitude Φ as given in Eq. (9) is gaussian, the two-photon amplitude Φ defined in Eq. (30) takes also a gaussian form, that can be found in Appendix A [Eq. (A10)].

Photon flux N_s in the signal field is then determined along the formula [19]

$$N_s(\tau_s) = \hbar\omega_s^0 \int_{-\infty}^{\infty} d\tau_i |\Phi(\tau_s, \tau_i)|^2, \quad (31)$$

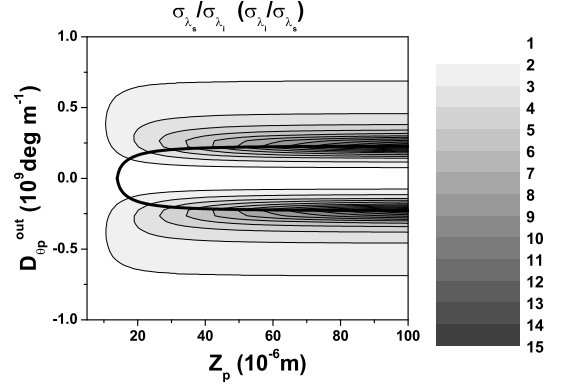


FIG. 3: Contour plot of ratio $\sigma_{\lambda_i}/\sigma_{\lambda_s}$ of spectral widths of signal- and idler-field intensities as a function of parameter $D_{\theta_p}^{\text{out}}$ giving angular decomposition of pump-beam frequencies outside the waveguide and pump-beam transverse width Z_p is shown. Ratio $\sigma_{\lambda_i}/\sigma_{\lambda_s}$ is plotter for $D_{\theta_p}^{\text{out}} < 0$. The bold curve indicating spectrally uncorrelated states is given using the formula in Eq. (55) later. We have $D_{\theta_p}^{\text{out}} = \tilde{D}_{\theta_p}^{\text{out}}(\omega_p^0)^2/(2\pi c)$, $\tilde{D}_{\theta_p}^{\text{out}} = [n_0(\omega_p^0) \cos(\theta_p^0)]/\cos(\theta_p^{\text{out}})\tilde{D}_{\theta_p} + \sin(\theta_p^0)/\cos(\theta_p^{\text{out}}) dn_0(\omega_p)/d\omega_p|_{\omega_p=\omega_p^0}$ and $\theta_p^{\text{out}} = \arcsin[n_0(\omega_p^0) \sin(\theta_p^0)]$; $\tau_p = 1 \times 10^{-13}$ s, values of the other parameters are given in Fig. 2.

and attains the following gaussian form;

$$N_s(\tau_s) = n_s \exp \left[-\frac{(\tau_s - \delta\tau_s^0)^2}{\sigma_{\tau_s}^2} \right]. \quad (32)$$

Considering a pump pulse without chirp ($a_p = 0$) and omitting contributions in Eq. (10) given by coefficients \mathcal{G}_s , \mathcal{G}_i , and \mathcal{G}_{si} , we arrive at the following simplified expressions:

$$n_s = |C_{\Phi}|^2 \frac{\sqrt{\pi} \hbar \omega_s^0 \tau_p Z_p}{\sqrt{\mathcal{D}_f}} \times \left[\frac{\tau_p^2}{2} + \frac{2}{\sigma_s^2} + \frac{Z_p^2 V_{ps}^2}{2} \right]^{-1/2}, \quad (33)$$

$$\sigma_{\tau_s} = \sqrt{\frac{\tau_p^2}{2} + \frac{2}{\sigma_s^2} + \frac{Z_p^2 V_{ps}^2}{2}}, \quad (34)$$

$$\delta\tau_s^0 = 0; \quad (35)$$

coefficient \mathcal{D}_f is given in Eq. (A11) in Appendix A. The formula in Eq. (34) shows that the signal-field temporal width σ_{τ_s} increases as the pump-pulse duration τ_p and pump-beam transverse width Z_p increase. Also the narrower the signal-field frequency filter, the greater the temporal width σ_{τ_s} .

Depending on pump-pulse duration τ_p and pump-beam transverse width Z_p width σ_{τ_s} of the signal-field intensity profile spreads from several tens to several hundreds of fs (see Fig. 4). Width σ_{τ_s} of the signal-field intensity temporal profile has to be greater than that characterizing

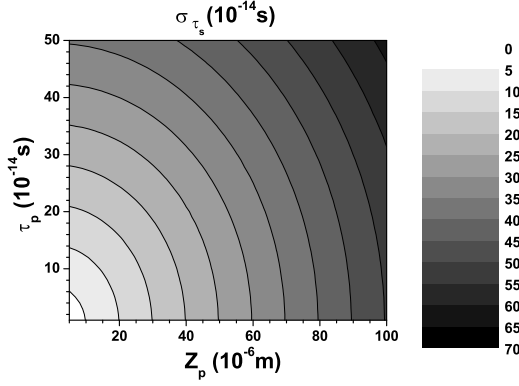


FIG. 4: Contour plot of temporal width σ_{τ_s} of signal-field photon flux as a function of pump-pulse duration τ_p and pump-beam transverse width Z_p is shown; values of the used parameters are given in Fig. 2.

the pump field ($\tau_p/\sqrt{2}$) as the expression in Eq. (34) confirms. Also the greater the pump-beam transverse width Z_p the greater the width σ_{τ_s} as a consequence of propagation of a signal photon along the waveguide. Angular decomposition of pump-beam frequencies (D_{θ_p}) can either broaden or shorten the pulsed photon fluxes N_s and N_i as follows from formulas in Eqs. (34) and (11).

Temporal and spectral widths of the down-converted fields are not independent provided that the pump pulse is not chirped ($a_p = 0$):

$$\frac{\sigma_{\omega_s} \sigma_{\tau_s}}{\sigma_{\omega_i} \sigma_{\tau_i}} = 1. \quad (36)$$

Considering the symmetric case ($\omega_s^0 = \omega_i^0$), cross spectrally pure pumping ($D_{\theta_p} = 0$) without chirp ($a_p = 0$), and no frequency filters ($\sigma_s, \sigma_i \rightarrow \infty$), the following relation for the product of temporal and spectral widths of the down-converted fields can be derived:

$$\sigma_{\omega_a} \sigma_{\tau_a} = \frac{1}{2} \left(\frac{v_a \tau_p}{Z_p} + \frac{Z_p}{v_a \tau_p} \right) \geq 1, \quad a = s, i. \quad (37)$$

Product $\sigma_{\omega_a} \sigma_{\tau_a}$ written in Eq. (37) goes to infinity for cw pumping.

Temporal properties as described by photon fluxes N_s and N_i are not accessible directly experimentally owing to very short time scales. Thus interferometric setups are needed to obtain these characteristics. Temporal overlap of the signal- and idler-photon wave-functions can be detected in a Hong-Ou-Mandel interferometer that provides a normalized coincidence-count rate R_n as a function of mutual time delay τ_l between the signal and idler photons [42]:

$$R_n(\tau_l) = 1 - \rho(\tau_l), \quad (38)$$

where

$$\rho(\tau_l) = \frac{1}{N} \int_{-\infty}^{\infty} dt_A \int_{-\infty}^{\infty} dt_B$$

$$\text{Re} \{ \Phi(t_A, t_B - \tau_l) \Phi^*(t_B, t_A - \tau_l) \} \quad (39)$$

and the number N of photons generated in 1 s is given by Eq. (18). Symbol Re means the real part of an argument. The shape of two-photon amplitude Φ thus determines the pattern of coincidence-count rate $R_n(\tau_l)$ as discussed, e.g., in [42].

Using the two-photon spectral amplitude Φ written in Eq. (9) the normalized coincidence-count rate R_n can be derived in the form:

$$R_n(\tau_l) = 1 - A \exp(-B\tau_l^2) \cos[(\omega_s^0 - \omega_i^0)\tau_l]. \quad (40)$$

Coefficients A and B are given as follows neglecting coefficients \mathcal{G}_s , \mathcal{G}_i , and \mathcal{G}_{si} [the general expressions can be found in Eqs. (A21) and (A22) in Appendix A]:

$$A|_{\sigma_s, \sigma_i \rightarrow \infty} = \left[1 + \frac{Z_p^2(1 + a_p^2)(V_{ps}^2 - V_{pi}^2)^2}{4\tau_p^2 V_{si}^2} \right]^{-1/2} \quad (41)$$

$$B = \left[\frac{2}{\sigma_s^2} + \frac{2}{\sigma_i^2} + \frac{Z_p^2 V_{si}^2}{2} \right]^{-1}. \quad (42)$$

Visibility V of a coincidence-count pattern described by the formula in Eq. (40) and defined along the expression ($R_{n,\min}$ gives a minimum value of R_n)

$$V = \frac{R_n(\tau_l \rightarrow \infty) - R_{n,\min}}{R_n(\tau_l \rightarrow \infty) + R_{n,\min}} \quad (43)$$

is obtained in the form:

$$V = \frac{A}{2 - A}. \quad (44)$$

For cw pumping ($\tau_p \rightarrow \infty$) and without frequency filters, coefficient $A \rightarrow 1$ and also visibility $V \rightarrow 1$. Visibility V equal to 1 is also reached for the symmetric case ($\omega_s^0 = \omega_i^0$ leads to $A = 1$).

On the other hand, coefficient B given in Eq. (42) determines width $\Delta\tau_l$ of the coincidence-count dip defined by the condition $R_n(\Delta\tau_l/2) = 1 - A/2$. This relation can be rewritten into a transcendent equation,

$$\frac{1}{2} - \exp\left(\frac{B\Delta\tau_l^2}{4}\right) \cos\left(\frac{\omega_s^0 - \omega_i^0}{2} \Delta\tau_l\right) = 0, \quad (45)$$

that has solution in the range $\Delta\tau_l \in (0, 2\pi/[\omega_s^0 - \omega_i^0])$. We note that oscillations at frequency $\omega_s^0 - \omega_i^0$ occur in the coincidence-count pattern of rate R_n . Coefficient B depends only on pump-beam transverse width Z_p and widths σ_s and σ_i of frequency filters. The narrower the frequency filters and the wider the pump-beam transverse width Z_p , the smaller the value of coefficient B and also the larger the width $\Delta\tau_l$ of normalized coincidence-count rate R_n . We can see that width $\Delta\tau_l$ of the coincidence-count dip does not depend on pump-pulse duration τ_p and pump-beam parameter D_{θ_p} . The reason is that a Hong-Ou-Mandel interferometer monitors only the difference of the signal- and idler-field frequencies $2\omega = \omega_s - \omega_i$

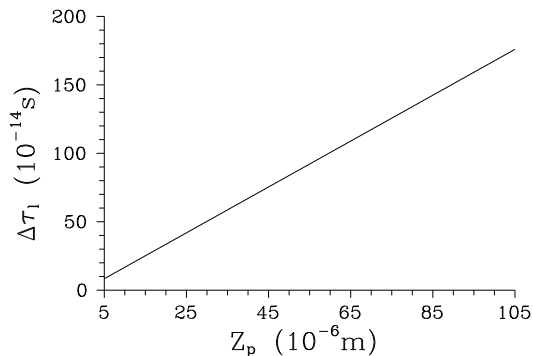


FIG. 5: Width $\Delta\tau_l$ of the dip in normalized coincidence-count rate R_n in a Hong-Ou-Mandel interferometer as it depends on pump-beam transverse width Z_p ; values of the used parameters are written in Fig. 2.

that depends only on pump-beam transverse width Z_p in the considered configuration [compare Eq. (14)].

Width $\Delta\tau_l$ of the coincidence-count dip can be controlled changing pump-beam transverse width Z_p in a broad range of its values, as documented in Fig. 5. This property may be useful in metrology applications (e.g., in measurement of modal dispersion of a waveguiding structure).

V. ENTANGLED AND SEPARABLE STATES

Entanglement between the signal- and idler-field frequencies can be conveniently quantified using entropy of entanglement [43, 44]. To determine entropy S_e of entanglement we have to decompose a two-photon spectral amplitude Φ into Schmidt decomposition [45]:

$$\Phi(\omega_s, \omega_i) = \sum_n \lambda_n \phi_{s,n}(\omega_s) \phi_{i,n}(\omega_i), \quad (46)$$

where λ_n are coefficients of the decomposition and functions $\phi_{s,n}(\omega_s)$ and $\phi_{i,n}(\omega_i)$ form the Schmidt basis. This decomposition assuming a gaussian two-photon spectral amplitude Φ is found in Appendix B and gives coefficients λ_n in the form of geometric progression:

$$\lambda_n = \sqrt{1 - \vartheta} \vartheta^{n/2}, \quad n = 0, 1, \dots, \infty. \quad (47)$$

Value of parameter ϑ is derived from values of parameters characterizing amplitude Φ using Eqs. (B8) and (B11) in Appendix B. We note that $\sum_n \lambda_n^2 = 1$ as a consequence of assumed normalization of the amplitude Φ ; $\int d\omega_s \int d\omega_i |\Phi(\omega_s, \omega_i)|^2 = 1$.

Entanglement between the signal- and idler-field frequencies can be determined using entropy S_e derived from eigenvalues λ_n of the Schmidt decomposition,

$$S_e = - \sum_n \lambda_n^2 \log_2(\lambda_n^2); \quad (48)$$

symbol \ln_2 means logarithm of base 2. Using Eq. (47) we arrive at:

$$S_e = - \log_2(1 - \vartheta) - \frac{\vartheta \log_2(\vartheta)}{1 - \vartheta}. \quad (49)$$

As for possible values of entropy S_e , there are two boundary cases. If $\vartheta \rightarrow 1$ (also $P \rightarrow 0$ and $|e_2| = e_{2c}$) then all eigenvalues λ_n are equal, i.e. we have a maximally entangled state. On the other hand, if $\vartheta \rightarrow 0$ (also $P \rightarrow \infty$ and $e_{2c} \rightarrow 0$) there is only one nonzero eigenvalue λ_0 ; i.e. the two-photon spectral amplitude $\Phi(\omega_s, \omega_i)$ factorizes and describes a separable state useful, e.g., in linear quantum computation [24].

A. Entangled states

Entangled states with high values of entropy S_e of entanglement are generated if either pump-pulse duration τ_p is short or pump-beam transverse width Z_p is narrow, as the analysis contained in Appendix B shows. The shorter the pump-pulse duration τ_p the greater the value of entropy S_e . The narrower the pump-beam transverse width Z_p the greater the value of entropy S_e . Also the wider the widths σ_s and σ_i of frequency filters the greater the values of entropy S_e .

On the other hand, widths σ_{ω_s} and σ_{ω_i} of the signal- and idler-field intensity spectra increase with decreasing pump-pulse duration τ_p and pump-beam transverse width Z_p . The used frequency filters make these spectra narrower. Comparing qualitatively this behavior with that of entropy S_e of entanglement described above, we can conclude that the wider the spectra of the signal and idler fields, the better the entanglement of the signal and idler fields.

Instead of characterizing entanglement by entropy S_e we can judge it by a minimum number n_{\min} of eigenfunctions (modes) from the Schmidt basis that restore a two-photon spectral amplitude Φ with probability p_{\min} . The number n_{\min} satisfies the following inequalities:

$$\sum_{n=0}^{n_{\min}-1} \lambda_n^2 \leq p_{\min} \wedge \sum_{n=0}^{n_{\min}} \lambda_n^2 \geq p_{\min}. \quad (50)$$

The value of probability p_{\min} should be chosen with respect to the precision of measurement.

For the considered waveguide, entropy S_e of entanglement as well as minimum number n_{\min} of modes are shown in Fig. 6 as they depend on pump-pulse duration τ_p and pump-beam transverse width Z_p . We can see in Fig. 6 that entanglement of the signal and idler fields is rather weak in a broad area around the bold curve characterizing spectrally uncorrelated (separable) states and so we can approximate the generated state by a separable two-photon spectral amplitude Φ . Entangled states for which several modes in the Schmidt decomposition are necessary occur on the borders of the contour plot, i.e. where the quantity $\tau_p v_s / Z_p$ considerably differs from one

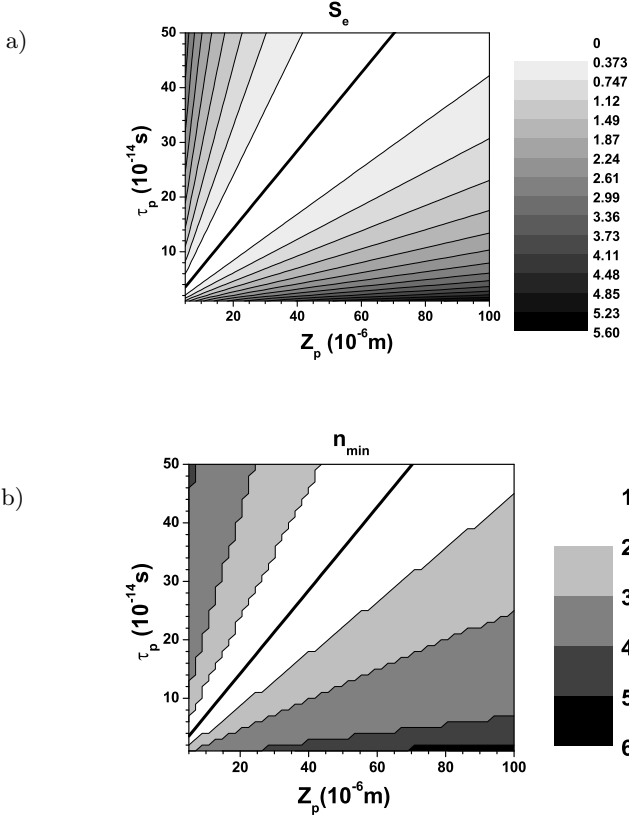


FIG. 6: Contour plots of entropy S_e of entanglement (a) and minimum number n_{\min} of modes in Schmidt decomposition ($p_{\min} = 0.95$) (b) as they depend on pump-pulse duration τ_p and pump-beam transverse width Z_p ; bold curves in the middle of the plots are given by the condition in Eq. (53) for spectrally uncorrelated states; values of the used parameters are given in Fig. 2.

[see Eq. (56) later]. Wide intensity spectra occur in this region (compare Fig. 2).

The narrower the frequency filters the lower the values of entropy S_e and thus the weaker the entanglement between the down-converted fields, as demonstrated in Fig. 7. Assuming $p_{\min} = 0.95$ and values of the waveguide parameters appropriate for Fig. 7, filters narrower than 12 nm transform the down-converted fields into a separable state whereas two independent modes are sufficient for wider filters.

B. Spectrally uncorrelated (separable) states

The condition for a separable state derived from the formula in Eq. (49), $e_{2c} = 0$, is fulfilled provided that $f_{2si} = 0$ as follows from the definition of coefficient e_{2c} in Eq. (B4) in Appendix B. Separability of the two-photon spectral amplitude Φ written in Eq. (9) is clearly visible in this case and shows that separable states are generated

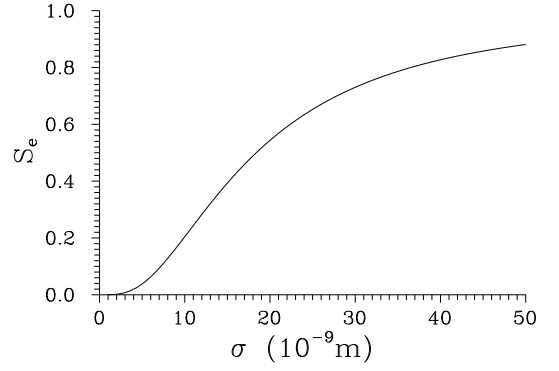


FIG. 7: Entropy S_e of entanglement as a function of width σ ($\sigma_s = \sigma_i = \sigma$) of frequency filters in nm; $\tau_p = 1 \times 10^{-13}$ s, $Z_p = 5 \times 10^{-6}$ m, $p_{\min} = 0.95$ and values of the other parameters are written in Fig. 2.

only provided that the axes in which the quadratic form given in Eq. (9) is diagonal coincide with the ω_s and ω_i axes. Eigenvalues $\mu_{1,2}$ of the quadratic form written in the second line of Eq. (9) are given as follows:

$$\mu_{1,2} = \frac{f_{2s} + f_{2i} \pm \sqrt{(f_{2s} - f_{2i})^2 + f_{2si}^2}}{2}, \quad (51)$$

whereas angle ψ_{si} giving declination of the axes of the diagonal quadratic form from the ω_s and ω_i axes is written as:

$$\tan(\psi_{si}) = \frac{f_{2s} - f_{2i} \pm \sqrt{(f_{2s} - f_{2i})^2 + f_{2si}^2}}{f_{2si}}. \quad (52)$$

The limit $f_{2si} \rightarrow 0$ in Eq. (52) leads to $\psi_{si} = 0$, i.e. the axes of diagonal quadratic form coincide with the ω_s and ω_i axes.

Substituting expressions in Eqs. (10) and (11) into the separability condition $f_{2si} = 0$ we arrive at:

$$\frac{\tau_p^2}{1 + ia_p} + Z_p^2 \left[\frac{\sin(\theta_p^0)}{v_p} + k_p^0 \cos(\theta_p^0) \tilde{D}_{\theta_p} - \frac{1}{v_s} \right] \times \left[\frac{\sin(\theta_p^0)}{v_p} + k_p^0 \cos(\theta_p^0) \tilde{D}_{\theta_p} + \frac{1}{v_i} \right] + 2\mathcal{G}_{si} = 0. \quad (53)$$

Assuming fixed values for pump-pulse duration τ_p and pump-beam transverse width Z_p and no chirp ($a_p = 0$) the condition in Eq. (53) represents a quadratic equation for parameter \tilde{D}_{θ_p} of angular decomposition of pump-beam frequencies and its solution takes the form:

$$\left(\tilde{D}_{\theta_p} \right)_{1,2} = \frac{1}{2k_p^0 \cos(\theta_p^0)} \left[-\frac{2 \sin(\theta_p^0)}{v_p} + \frac{1}{v_s} - \frac{1}{v_i} \pm \sqrt{\left(\frac{1}{v_s} + \frac{1}{v_i} \right)^2 - 4 \frac{\tau_p^2}{Z_p^2} - 8 \frac{\mathcal{G}_{si}}{Z_p^2}} \right]. \quad (54)$$

Solution for \tilde{D}_{θ_p} written in Eq. (54) exists only when argument of the square root in Eq. (54) is non-negative.

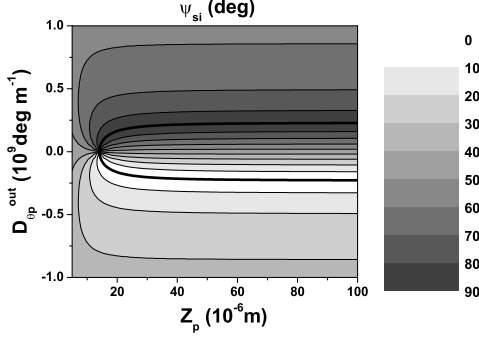


FIG. 8: Angle ψ_{si} giving orientation of axes of the diagonal quadratic form of two-photon spectral amplitude Φ with respect to the ω_s and ω_i axes as it depends on pump-beam transverse width Z_p and parameter $D_{\theta_p}^{\text{out}}$ giving angular decomposition of pump-beam frequencies outside the waveguide (for its determination, see Fig. 3). The bold curve indicates spectrally uncorrelated states and is given by the formula in Eq. (55); $\tau_p = 1 \times 10^{-13}$ s, values of the other parameters are the same as in Fig. 2.

Thus, there is a lower limit for possible values of pump-beam transverse width Z_p keeping pump-pulse duration τ_p fixed.

Considering the symmetric case ($\omega_s^0 = \omega_i^0$) and neglecting coefficient \mathcal{G}_{si} , the formula in Eq. (54) for \tilde{D}_{θ_p} simplifies:

$$\left(\tilde{D}_{\theta_p}\right)_{1,2} = \pm \frac{1}{k_p^0} \sqrt{\frac{1}{v_s^2} - \frac{\tau_p^2}{Z_p^2}} \quad (55)$$

and is valid provided that $Z_p \geq v_s \tau_p$. If the pump beam is cross spectrally pure, i.e. $\tilde{D}_{\theta_p} = 0$, the following condition assures the generation of a separable state:

$$\frac{\tau_p}{Z_p} = \frac{1}{v_s}. \quad (56)$$

Changing values of parameters τ_p , Z_p , and \tilde{D}_{θ_p} photon pairs with an arbitrary gaussian two-photon spectral amplitude Φ can be generated [40]. An arbitrary orientation of axes of the diagonal quadratic form of two-photon amplitude Φ can be reached changing the value of parameter \tilde{D}_{θ_p} of angular decomposition of pump-beam frequencies, as demonstrated in Fig. 8. Parameters τ_p and Z_p then control spread of the two-photon spectral amplitude Φ along the axes given by angles ψ_{si} and $\psi_{si} + \pi/2$. Comparison of graphs in Figs. 3 and 8 with special attention to frequency uncorrelated states leads to the conclusion that the greater the pump-beam transverse width Z_p the greater the ratio $\sigma_{\omega_s}/\sigma_{\omega_i}$ of intensity spectral widths of the down-converted fields. Such states have been found useful in quantum communication protocols.

VI. EXPERIMENTAL DETERMINATION OF ENTROPY OF ENTANGLEMENT

If the pump field is not chirped ($a_p = 0$), a generated photon pair is described by a two-photon spectral amplitude Φ in a gaussian form written in Eq. (9) that, apart from central frequencies, is specified by three real parameters. These parameters can be experimentally determined measuring widths of the signal- (σ_{ω_s}) and idler-field (σ_{ω_i}) intensity spectra and width $\Delta\tau_l$ of coincidence-count pattern in a Hong-Ou-Mandel interferometer, as shown below.

Coefficient B describing width of the coincidence-count dip in the Hong-Ou-Mandel interferometer can be obtained by fitting the experimental curve $R_n(\tau_l)$ using the prescription written in Eq. (40). The measured widths σ_{ω_s} and σ_{ω_i} of signal- and idler-field intensity spectra provide coefficient F [for definition, see Eq. (A9) in Appendix A]:

$$F = \frac{\sigma_{\omega_i}^2}{\sigma_{\omega_s}^2}. \quad (57)$$

Further, Eqs. (A9) and (A22) in Appendix A can be recast into the form:

$$\begin{aligned} f_{2i}^r &= \frac{f_{2s}^r}{F}, \\ f_{2si}^r &= \frac{F+1}{F} f_{2s}^r - \frac{1}{2B}. \end{aligned} \quad (58)$$

Substitution of Eqs. (58) into Eqs. (A2) and (A5) in Appendix A leads to a quadratic equation for coefficient f_{2s}^r :

$$-\frac{(F-1)^2}{F} (f_{2s}^r)^2 + \left(\frac{F+1}{B} - \frac{2}{\sigma_{\omega_s}^2}\right) f_{2s}^r - \frac{F}{4B^2} = 0. \quad (59)$$

Solution of Eq. (59) gives the value of coefficient f_{2s}^r . For the symmetric case ($\omega_s^0 = \omega_i^0$), $F = 1$ and we have

$$f_{2s}^r = \frac{\sigma_{\omega_s}^2}{8B(\sigma_{\omega_s}^2 - B)}. \quad (60)$$

Values of coefficients f_{2i} and f_{2si} are then given by formulas in Eqs. (58). Coefficients f_{1s} and f_{1i} occurring in Eq. (9) give only shifts on the frequency axes ω_s and ω_i and can be neglected. Also coefficient f_0 in Eq. (9) giving normalization can be omitted.

Knowing values of coefficients f_{2s} , f_{2i} , and f_{2si} , entropy S_e of entanglement can finally be determined along the formulas given in Eqs. (B4), (B11), (B8), and (49).

VII. CONCLUSIONS

Properties of the down-converted fields can be controlled in wide ranges of values of characteristic parameters using pump-pulse duration, pump-beam transverse

width, and angular decomposition of pump-beam frequencies in a waveguide with counter-propagating down-converted fields and transverse pumping. Widths of intensity spectra of the down-converted fields may vary from nanometers to tens of nanometers. Durations of the down-converted pulsed fields extend from tens of fs to several ps. Both entangled and separable (spectrally uncorrelated) photon pairs useful in linear quantum computation can be generated. Also attainable widths of a coincidence-count dip in a Hong-Ou-Mandel interferometer lie in a broad interval that is of interest in metrology applications. Using the measured spectral widths of the signal and idler fields and width of the coincidence-count dip, entropy of entanglement as well as parameters characterizing a two-photon spectral amplitude can be obtained.

The considered nonlinear waveguide is promising as a versatile source of photon pairs in near future provided that efficiency of the nonlinear process is increased.

Acknowledgments

The author thanks V. Peřinová and A. Lukš for their help with calculations and M. Centini for useful discussions. Support by projects IAA 100100713 of GA AS CR, 1M06002, COST OC P11.003, and AVOZ 10100522 of the Czech Ministry of Education is acknowledged.

APPENDIX A: GENERAL FORMULAS FOR PHYSICAL QUANTITIES CHARACTERIZING THE EMITTED PHOTON PAIRS

1. Spectral properties

Substitution of the general form of two-photon spectral amplitude Φ as given in Eq. (9) into Eq. (18) results in the following expression for the number N of generated photon pairs in 1 s:

$$N = |C_\Phi|^2 \exp(-2f_0) \frac{\pi Z_p \tau_p}{(1 + a_p^2) \sqrt{\mathcal{D}_{fr}}} \mathcal{E}_{fr}, \quad (\text{A1})$$

where

$$\mathcal{D}_{fr} = 4f_{2s}^r f_{2i}^r - (f_{2si}^r)^2 \quad (\text{A2})$$

and

$$\mathcal{E}_{fr} = \exp\left(2 \frac{f_{2s}^r f_{1i}^2 + f_{2i}^r f_{1s}^2 - f_{2si}^r f_{1s} f_{1i}}{\mathcal{D}_{fr}}\right). \quad (\text{A3})$$

Superscript r indicates the real part of a given complex coefficient.

A gaussian signal-field intensity spectrum $S_s(\omega_s)$ as written in Eq. (23) is determined by its amplitude s_s ,

width σ_{ω_s} , and shift $\delta\omega_s^0$ of the center that are given in general by the following expressions:

$$s_s = |C_\Phi|^2 \exp(-2f_0) \frac{\sqrt{\pi} \hbar \omega_s \tau_p Z_p}{\sqrt{2}(1 + a_p^2)} \frac{1}{\sqrt{f_{2i}^r}} \mathcal{E}_{fr}, \quad (\text{A4})$$

$$\sigma_{\omega_s} = \sqrt{\frac{2f_{2i}^r}{\mathcal{D}_{fr}}}, \quad (\text{A5})$$

$$\delta\omega_s^0 = -\frac{2f_{2i}^r f_{1s} - f_{2si}^r f_{1i}}{\mathcal{D}_{fr}}, \quad (\text{A6})$$

where coefficients \mathcal{D}_{fr} and \mathcal{E}_{fr} are given in Eqs. (A2) and (A3). Expressions for amplitude s_i , width σ_{ω_i} , and shift $\delta\omega_i^0$ belonging to the idler-field intensity spectrum $S_i(\omega_i)$ can be obtained from those written in Eqs. (A4–A6) by an exchange of indices s and i .

Relations among parameters of the signal- and idler-field intensity spectra can be established for a two-photon spectral amplitude Φ written in Eq. (9):

$$s_i = \frac{\omega_i^0}{\omega_s^0} \sqrt{F} s_s, \quad (\text{A7})$$

$$\sigma_{\omega_i} = \frac{1}{\sqrt{F}} \sigma_{\omega_s}. \quad (\text{A8})$$

Symbol F ,

$$F = \frac{f_{2s}^r}{f_{2i}^r}, \quad (\text{A9})$$

gives the ratio of parameters that characterize a gaussian two-photon spectral amplitude Φ .

2. Temporal properties

Substituting the expression in Eq. (9) for two-photon spectral amplitude $\Phi(\omega_s, \omega_i)$ into the definition of amplitude $\Phi(\tau_s, \tau_i)$ occurring in Eq. (30), we arrive at

$$\begin{aligned} \Phi(\tau_s, \tau_i) &= C_\phi \exp(-f_0) \sqrt{\frac{Z_p \tau_p}{(1 + a_p^2) \mathcal{D}_f}} \\ &\times \exp\left[-\frac{f_{2i}(\tau_s - i f_{1s})^2 + f_{2s}(\tau_i - i f_{1i})^2}{\mathcal{D}_f}\right] \\ &\times \exp\left[\frac{f_{2si}(\tau_s - i f_{1s})(\tau_i - i f_{1i})}{\mathcal{D}_f}\right] \end{aligned} \quad (\text{A10})$$

and

$$\mathcal{D}_f = 4f_{2s} f_{2i} - f_{2si}^2. \quad (\text{A11})$$

Parameters of the gaussian form of signal-field photon flux N_s written in Eq. (32) [amplitude n_s , width σ_{τ_s} , and shift $\delta\tau_s^0$] are given for the general form of two-photon spectral amplitude Φ in Eq. (9) by the following formulas, similarly as in the case of intensity spectra:

$$n_s = |C_\Phi|^2 \exp(-2t_0) \frac{\sqrt{\pi} \hbar \omega_s^0 \tau_p Z_p}{\sqrt{2}(1 + a_p^2)} \frac{1}{|\mathcal{D}_f|} \frac{1}{\sqrt{t_{2i}}} \mathcal{E}_t,$$

$$(A12)$$

$$\sigma_{\tau_s} = \sqrt{\frac{2t_{2i}}{\mathcal{D}_t}}, \quad (A13)$$

$$\delta\tau_s^0 = -\frac{2t_{2i}t_{1s} - t_{2si}t_{1i}}{\mathcal{D}_t}, \quad (A14)$$

and

$$\mathcal{D}_t = 4t_{2s}t_{2i} - t_{2si}^2, \quad (A15)$$

$$\mathcal{E}_t = \exp\left(2\frac{t_{2s}t_{1i}^2 + t_{2i}t_{1s}^2 - t_{2si}t_{1s}t_{1i}}{\mathcal{D}_t}\right). \quad (A16)$$

Coefficients t occurring in the above Eqs. (A12 —A16) are given as:

$$\begin{aligned} t_{2s} &= \text{Re}\{f_{2i}/\mathcal{D}_f\}, \\ t_{2i} &= \text{Re}\{f_{2s}/\mathcal{D}_f\}, \\ t_{2si} &= -\text{Re}\{f_{2si}/\mathcal{D}_f\}, \\ t_{1s} &= \text{Im}\{(2f_{2i}f_{1s} - f_{2si}f_{1i})/\mathcal{D}_f\}, \\ t_{1i} &= \text{Im}\{(2f_{2s}f_{1i} - f_{2si}f_{1s})/\mathcal{D}_f\}, \\ t_0 &= f_0 - \text{Re}\{(f_{2i}f_{1s}^2 + f_{2s}f_{1i}^2 - f_{2si}f_{1s}f_{1i})/\mathcal{D}_f\}; \end{aligned} \quad (A17)$$

Re (Im) denotes a real (imaginary) part of an expression. Similarly as in the case of spectral properties, relations among parameters of the signal and idler fields can be derived:

$$n_i = \frac{\omega_i^0}{\omega_s^0} \sqrt{T} n_s, \quad (A18)$$

$$\sigma_{\tau_i} = \frac{1}{\sqrt{T}} \sigma_{\tau_s}. \quad (A19)$$

Parameter T ,

$$T = \frac{t_{2i}}{t_{2s}}, \quad (A20)$$

gives the ratio of parameters that characterize a gaussian two-photon amplitude Φ in the time domain. If the pulsed pump field is not chirped, we have $T = 1/F$.

Coefficients A and B characterizing a coincidence-count pattern in a Hong-Ou-Mandel interferometer as given in Eq. (40) are determined for the general form of two-photon spectral amplitude Φ as follows:

$$A = \sqrt{\frac{\mathcal{D}_{fr}}{(f_{2s} + f_{2i}^*)^2 - (f_{2si}^r)^2}} \exp\left[\frac{(f_{1s} + f_{1i})^2}{2(f_{2s} + f_{2i}^* + f_{2si})}\right] \times \mathcal{E}_{fr}^{-1}, \quad (A21)$$

$$B = \frac{1}{2(f_{2s} + f_{2i}^* - f_{2si})}, \quad (A22)$$

and coefficients \mathcal{D}_{fr} and \mathcal{E}_{fr} are given by formulas in Eqs. (A2) and (A3).

APPENDIX B: SCHMIDT DECOMPOSITION OF TWO-PHOTON SPECTRAL AMPLITUDE Φ

In order to determine Schmidt decomposition of two-photon spectral amplitude Φ as given in Eq. (46) we need reduced statistical operators belonging to the signal and idler fields. Statistical operator $\hat{\rho}_s$ of the signal field can be written in the form:

$$\hat{\rho}_s = \int_{-\infty}^{\infty} d\omega'_s \int_{-\infty}^{\infty} d\omega_s \Psi_s(\omega'_s, \omega_s) \hat{a}_s^\dagger(\omega'_s) |\text{vac}\rangle \langle \text{vac}| \hat{a}_s(\omega_s). \quad (B1)$$

Weighting function Ψ_s determined along the formula

$$\Psi_s(\omega'_s, \omega_s) = \int_{-\infty}^{\infty} d\omega_i \Phi(\omega'_s, \omega_i) \Phi^*(\omega_s, \omega_i) \quad (B2)$$

takes the following form using Eq. (9) for the two-photon spectral amplitude Φ :

$$\begin{aligned} \Psi_s(\omega'_s, \omega_s) &= |\tilde{C}_\Psi|^2 \exp(-e_2 \omega_s^2 - e_2^* \omega_s'^2 + 2e_{2c} \omega_s \omega_s') \\ &\times \exp(e_1 \omega_s + e_1^* \omega_s'), \end{aligned} \quad (B3)$$

and

$$\begin{aligned} e_2 &= f_{2s} - \frac{f_{2si}^2}{8f_{2i}^r}, \\ e_{2c} &= \frac{|f_{2si}|^2}{8f_{2i}^r}, \\ e_1 &= f_{1s} - \frac{f_{1i}f_{2si}}{(f_{2i}^r)^2}. \end{aligned} \quad (B4)$$

Normalization constant \tilde{C}_Ψ introduced in Eq. (B3),

$$|\tilde{C}_\Psi|^2 = \sqrt{\frac{2(e_2^r - e_{2c})}{\pi}} \exp\left[-\frac{(e_1^r)^2}{2(e_2^r - e_{2c})}\right], \quad (B5)$$

guarantees normalization of the signal-field statistical operator $\hat{\rho}_s$ such that $\int_{-\infty}^{\infty} d\omega_s \Psi(\omega_s, \omega_s) = 1$. Statistical operator $\hat{\rho}_i$ of the idler field can be expressed similarly as that for the signal field.

Coefficients λ_n and functions $\phi_{s,n}$ and $\phi_{i,n}$ occurring in the Schmidt decomposition in Eq. (46) are given as solutions of the following integral equations:

$$\int_{-\infty}^{\infty} d\omega_a \Psi_a(\omega'_a, \omega_a) \phi_{a,n}(\omega_a) = \lambda_n^2 \phi_{a,n}(\omega'_a), \quad a = s, i. \quad (B6)$$

Using linear substitution the kernel Ψ_s in Eq. (B3) can be transformed into the form:

$$\Psi(x, y) = \exp[-(1+P)(x^2 + y^2) + 2xy] \quad (B7)$$

and

$$P = \frac{|e_2|}{e_{2c}} - 1. \quad (B8)$$

It can be shown [46] that the following functions ϕ_n obey the integral equation in Eq. (B6) for kernel Ψ defined in Eq. (B7):

$$\phi_n(x) = \sqrt{\frac{\sqrt{1-\vartheta^2}}{2^n n! \sqrt{\pi} \vartheta}} \exp\left(-\frac{1-\vartheta^2}{2\vartheta} x^2\right) \times H_n\left(\sqrt{\frac{1-\vartheta^2}{\vartheta}} x\right), \quad n = 0, 1, \dots, \infty; \quad (\text{B9})$$

symbols H_n denote Hermite polynomials. The corresponding eigenvalues λ_n^2 form a geometric progression:

$$\lambda_n^2 = \sqrt{\pi} \vartheta^n, \quad n = 0, 1, \dots, \infty \quad (\text{B10})$$

and parameter ϑ is given as follows:

$$\vartheta = 1 + P - \sqrt{P^2 + 2P}. \quad (\text{B11})$$

A maximally entangled state according to entropy S_e of entanglement determined in Eq. (49) is reached if all eigenvalues λ_n are equal, i.e. when $P \rightarrow 0$. To understand this condition, we express coefficient P defined in Eq. (B8) in terms of coefficients f :

$$P = \sqrt{1 + \frac{16f_{2i}^r}{|f_{2si}|^4} (4|f_{2s}|^2 f_{2i}^r - \text{Re}\{f_{2s} f_{2si}^{*2}\})} - 1. \quad (\text{B12})$$

It can be shown that coefficient P goes to zero if coefficient \mathcal{D}_f defined in Eq. (A11) goes to zero too. Provided that coefficients \mathcal{G}_s , \mathcal{G}_i , and \mathcal{G}_{si} can be omitted, the condition $\mathcal{D}_f = 0$ is fulfilled only in the limit $\tau_p \rightarrow 0$ and $Z_p \rightarrow 0$. For this reason, we investigate the behavior of coefficient \mathcal{D}_f with respect to pump-pulse duration τ_p , pump-beam transverse width Z_p , and widths σ_s and σ_i of frequency filters in the area around $\tau_p = 0$ or $Z_p = 0$.

For fixed values of Z_p , σ_s , and σ_i and around $\tau_p = 0$ the following equality holds:

$$\left. \frac{\partial \mathcal{D}_f}{\partial (\tau_p^2)} \right|_{Z_p, \sigma_s, \sigma_i} = \frac{1}{1 + ia_p} \left[\frac{V_{si}^2 Z_p^2}{4} + \frac{1}{\sigma_s^2} + \frac{1}{\sigma_i^2} \right]$$

$$+ \mathcal{G}_s + \mathcal{G}_i - \mathcal{G}_{si}. \quad (\text{B13})$$

Also fixing values of τ_p , σ_s , and σ_i and being around $Z_p = 0$ we arrive at:

$$\left. \frac{\partial \mathcal{D}_f}{\partial (Z_p^2)} \right|_{\tau_p, \sigma_s, \sigma_i} = \frac{1}{1 + ia_p} \frac{V_{si}^2 \tau_p^2}{4} + V_{ps}^2 \left(\frac{1}{\sigma_i^2} + \mathcal{G}_i \right) + V_{pi}^2 \left(\frac{1}{\sigma_s^2} + \mathcal{G}_s \right) - V_{ps} V_{pi} \mathcal{G}_{si}. \quad (\text{B14})$$

If $(dn_0(\omega_a)/d\omega_a|_{\omega_a=\omega_a^0})\omega_a^0 \ll n_a$ for $a = s, i$ then $g_{2si} = 2\sqrt{g_{2s}g_{2i}}$ and the derivatives in Eqs. (B13) and (B14) are positive ($a_p = 0$ is assumed). This means that if the value of pump-pulse duration τ_p is small [lower than that given by the condition in Eq. (53)] the shorter the pump-pulse duration τ_p the more the down-converted fields are entangled. Similarly it holds for sufficiently small values of pump-beam transverse width Z_p that the narrower the pump-beam transverse width Z_p the more the down-converted fields are entangled.

We get the following expressions for derivatives of coefficient \mathcal{D}_f with respect to widths σ_s and σ_i of frequency filters:

$$\left. \frac{\partial \mathcal{D}_f}{\partial (\sigma_s^2)} \right|_{\tau_p, Z_p} = -\frac{1}{\sigma_s^4} \left[\frac{\tau_p^2}{1 + ia_p} + V_{pi}^2 Z_p^2 + \frac{1}{\sigma_i^2} + \mathcal{G}_i \right],$$

$$\left. \frac{\partial \mathcal{D}_f}{\partial (\sigma_i^2)} \right|_{\tau_p, Z_p} = -\frac{1}{\sigma_i^4} \left[\frac{\tau_p^2}{1 + ia_p} + V_{ps}^2 Z_p^2 + \frac{1}{\sigma_s^2} + \mathcal{G}_s \right]. \quad (\text{B15})$$

For our waveguide, $\mathcal{G}_s > 0$ and $\mathcal{G}_i > 0$ and this means that the derivatives of coefficient \mathcal{D}_f written in Eqs. (B15) are negative ($a_p = 0$ is assumed). Thus the wider the frequency filters, the smaller the value of coefficient \mathcal{D}_f and the more the down-converted fields are entangled.

-
- [1] C.K. Hong, Z.Y. Ou, and L. Mandel, Phys. Rev. Lett. **59**, 2044 (1987).
[2] L. Mandel, E. Wolf, *Optical Coherence and Quantum Optics* (Cambridge Univ. Press. Cambridge, 1995).
[3] D. Bouwmeester, J.-W. Pan, K. Mattle, M. Eibl, H. Weinfurter, and A. Zeilinger, Nature **390**, 575 (1997).
[4] F. De Martini, V. Mussi, and F. Bovino, Opt. Commun. **179**, 581 (2000).
[5] J. Peřina, Z. Hradil, and B. Jurčo, *Quantum Optics and Fundamentals of Physics* (Kluwer, Dordrecht, 1994).
[6] F.A. Bovino, G. Castagnoli, A. Ekert, P. Horodecki, C.M. Alves, and A.V. Sergienko, Phys. Rev. Lett. **95**, 240407 (2005).
[7] D. Bouwmeester, J.-W. Pan, M. Daniell, H. Weinfurter, and A. Zeilinger, Phys. Rev. Lett. **82**, 1345 (1999).
[8] D. Bruß and N. Lütkenhaus, in *Applicable Algebra in Engineering, Communication and Computing* Vol. 10 (Springer, Berlin, 2000); p. 383.
[9] A. Migdall, Physics Today **52** (1), 41 (1999).
[10] P.G. Kwiat, E. Waks, A.G. White, I. Appelbaum, and P.H. Eberhard, Phys. Rev. A **60**, R773 (1999).
[11] Y. Nambu, K. Usami, Y. Tsuda, K. Matsumoto, and K. Nakamura, Phys. Rev. A **66**, 033816 (2002).
[12] C.E. Kuklewicz, M. Fiorentino, G. Messin, F.N.C. Wong, and J. Shapiro, Opt. Express **13**, 127 (2005).
[13] S. Carrasco, J.P. Torres, L. Torner, A.V. Sergienko, B.E.A. Saleh, and M.C. Teich, Phys. Rev. A **70**, 043817 (2004).

- [14] H.G. de Chatellus, A.V. Sergienko, B.E.A. Saleh, M.C. Teich, and G. Di Giuseppe, *Opt. Express* **14**, 10060 (2006).
- [15] S.E. Harris, *Phys. Rev. Lett.* **98**, 063602 (2007).
- [16] X. Li, P.L. Voss, J.E. Sharping, and P. Kumar, *Phys. Rev. Lett.* **94**, 053601 (2005).
- [17] J. Fulconis, O. Alibart, W.J. Wadsworth, P. S. Russell, and J. G. Rarity, *Opt. Express* **13**, 7572 (2005).
- [18] M. Centini, J. Peřina Jr., L. Sciscione, C. Sibilial, M. Scalora, M.J. Bloemer, and M. Bertolotti, *Phys. Rev. A* **72**, 033806 (2005).
- [19] J. Peřina Jr., M. Centini, C. Sibilial, M. Bertolotti, and M. Scalora, *Phys. Rev. A* **73**, 033823 (2006).
- [20] V. Giovannetti, L. Maccone, J.H. Shapiro, and F.N.C. Wong, *Phys. Rev. Lett.* **88**, 183602 (2002).
- [21] V. Giovannetti, L. Maccone, J.H. Shapiro, and F.N.C. Wong, *Phys. Rev. A* **66**, 043813 (2002).
- [22] O. Kuzucu, M. Fiorentino, M.A. Albota, F.N.C. Wong, and F.X. Kaertner, *Phys. Rev. Lett.* **94**, 083601 (2005).
- [23] V. Giovannetti, S. Lloyd, L. Maccone, and F.N.C. Wong, *Phys. Rev. Lett.* **87**, 117902 (2001).
- [24] A.B. U'Ren, K. Banaszek, and I.A. Walmsley, *Quantum Inf. Comp.* **3**, 480 (2003).
- [25] A.B. U'Ren, C. Silberhorn, K. Banaszek, I.A. Walmsley, R.K. Erdmann, W.P. Grice, and M.G. Raymer, *Laser Phys.* **15**, 146 (2005).
- [26] W.P. Grice, A.B. U'Ren, and I.A. Walmsley, *Phys. Rev. A* **64**, 063815 (2001).
- [27] S. Carrasco, A.V. Sergienko, B.E.A. Saleh, M.C. Teich, J.P. Torres, and L. Torner, *Phys. Rev. A* **73**, 063802 (2006).
- [28] J.P. Torres, F. Macia, S. Carrasco, and L. Torner, *Opt. Lett.* **30**, 314 (2005).
- [29] J.P. Torres, M.W. Mitchell, and M. Hendrych, *Phys. Rev. A* **71**, 022320 (2005).
- [30] A.B. U'Ren, R. Erdmann, and I.A. Walmsley, *J. Mod. Opt.* **52**, 2197 (2005).
- [31] A.B. U'Ren, R.K. Erdmann, M. de la Cruz-Gutierrez, and I.A. Walmsley, *Phys. Rev. Lett.* **97**, 223602 (2006).
- [32] J. Peřina Jr., M. Centini, C. Sibilial, M. Bertolotti, and M. Scalora, *Phys. Rev. A* **75**, 013805 (2007).
- [33] Y.J. Ding, S.J. Lee, and J.B. Khurgin, *Phys. Rev. Lett.* **75**, 429 (1995).
- [34] A. De Rossi and V. Berger, *Phys. Rev. Lett.* **88**, 043901 (2002).
- [35] M.C. Booth, M. Atature, G. Di Giuseppe, B.E.A. Saleh, A.V. Sergienko, and M.C. Teich, *Phys. Rev. A* **66**, 023815 (2002).
- [36] Z.D. Walton, M.C. Booth, A.V. Sergienko, B.E.A. Saleh, and M.C. Teich, *Phys. Rev. A* **67**, 053810 (2003).
- [37] M. Ravaro, Y. Seurin, S. Ducci, G. Leo, V. Berger, A. De Rossi, and G. Assanto, *J. Appl. Phys.* **98**, 063103 (2005).
- [38] L. Sciscione, M. Centini, C. Sibilial, M. Bertolotti, and M. Scalora, *Phys. Rev. A* **74**, 013815 (2006).
- [39] L. Lanco, S. Ducci, J.-P. Likforman, X. Marcadet, J.A.W. van Houwelingen, H. Zbinden, G. Leo, and V. Berger, *Phys. Rev. Lett.* **97**, 173901 (2006).
- [40] Z.D. Walton, A.V. Sergienko, B.E.A. Saleh, and M.C. Teich, *Phys. Rev. A* **70**, 052317 (2004).
- [41] A.W. Snyder and J.D. Love, *Optical Waveguide Theory*, (Chapman & Hall, London, 1983).
- [42] J. Peřina Jr., A.V. Sergienko, B.M. Jost, B.E.A. Saleh, M.C. Teich, *Phys. Rev. A* **59**, 2359 (1999).
- [43] C.K. Law, I.A. Walmsley, and J.H. Eberly, *Phys. Rev. Lett.* **84**, 5304 (2000).
- [44] C.K. Law and J.H. Eberly, *Phys. Rev. Lett.* **92**, 127903 (2004).
- [45] S. Parker, S. Bose, and M.B. Plenio, *Phys. Rev. A* **61**, 032305 (2000).
- [46] V. Peřinová and A. Lukš, private communication.